ARL-TR-8034 ● JUN 2017

US Army Research Laboratory

Optimization of In-Cylinder Pressure Filter for Engine Research

by Kenneth S Kim, Michael T Szedlmayer, Kurt M Kruger, and Chol-Bum M Kweon

NOTICES

Disclaimers

The findings in this report are not to be construed as an official Department of the Army position unless so designated by other authorized documents.

Citation of manufacturer's or trade names does not constitute an official endorsement or approval of the use thereof.

Destroy this report when it is no longer needed. Do not return it to the originator.

ARL-TR-8034 ● JUN 2017

US Army Research Laboratory

Optimization of In-Cylinder Pressure Filter for Engine Research

by Kenneth S Kim, Michael T Szedlmayer, Kurt M Kruger, and Chol-Bum M Kweon
Vehicle Technology Directorate, ARL

REPORT DOCUMENTATION PAGE

Form Approved
OMB No. 0704-0188

1. REPORT DATE *(DD-MM-YYYY)*	2. REPORT TYPE	3. DATES COVERED (From - To)
June 2017	Technical Report	June 2016–December 2016

4. TITLE AND SUBTITLE
Optimization of In-Cylinder Pressure Filter for Engine Research

5a. CONTRACT NUMBER

5b. GRANT NUMBER

5c. PROGRAM ELEMENT NUMBER

6. AUTHOR(S)
Kenneth S Kim, Michael T Szedlmayer, Kurt M Kruger, and Chol-Bum M Kweon

5d. PROJECT NUMBER

5e. TASK NUMBER

5f. WORK UNIT NUMBER

7. PERFORMING ORGANIZATION NAME(S) AND ADDRESS(ES)
US Army Research Laboratory
ATTN: RDRL-VTP
Aberdeen Proving Ground, MD 21005-5066

8. PERFORMING ORGANIZATION REPORT NUMBER
ARL-TR-8034

9. SPONSORING/MONITORING AGENCY NAME(S) AND ADDRESS(ES)

10. SPONSOR/MONITOR'S ACRONYM(S)

11. SPONSOR/MONITOR'S REPORT NUMBER(S)

12. DISTRIBUTION/AVAILABILITY STATEMENT
Approved for public release; distribution is unlimited.

13. SUPPLEMENTARY NOTES

14. ABSTRACT
Proper filtering of an engine's in-cylinder pressure is very important for analyzing combustion events. The objective of this study was to investigate and determine the optimal filter and its parameters for removing signal noise while retaining in-cylinder pressure characteristics of interest, for both normal and abnormal combustion events. A 4-cylinder direct-injection aviation diesel engine was instrumented to acquire in-cylinder pressure with a range of combustion events. Simple smoothing filters showed limited performance for an abnormal combustion event, resulting in biased in-cylinder pressure near start-of-combustion. The Savitzky-Golay filter, one of the simple smoothing filters, determined filtered in-cylinder pressure with high accuracy near start-of-combustion but underperformed in removing signal noise after start-of-combustion. Various linear continuous-time filters with frequency stop-band have advantages over simple smoothing filters in removing signal noise with magnitude response as a function of frequency. A number of linear continuous-time filters with different phase-response characteristics were investigated, and the optimal filter response and parameters were determined to effectively filter in-cylinder pressure of an aviation diesel engine. The Chebyshev filter with 5th-order polynomial and 0.001%-allowed ripples showed the best results in matching the raw signal near start-of-combustion and minimizing oscillations after start-of-combustion.

15. SUBJECT TERMS
engine, pressure, filter, combustion, analysis

16. SECURITY CLASSIFICATION OF:			17. LIMITATION OF ABSTRACT	18. NUMBER OF PAGES	19a. NAME OF RESPONSIBLE PERSON
a. REPORT	b. ABSTRACT	c. THIS PAGE			Kenneth S Kim
Unclassified	Unclassified	Unclassified	UU	38	19b. TELEPHONE NUMBER (Include area code) 410-278-9525

Contents

List of Figures iv

1. Introduction 1

2. Experimental Setup 2

3. Filtering Approaches 2

3.1 Simple Filters 3

3.2 Linear Continuous-Time Filter 5

3.2.1 Filter Comparison 5

3.2.2 Filter Optimization 7

4. Results and Discussion 9

4.1 Filtered In-Cylinder Pressure 9

4.2 Heat-Release-Rate Results using the New Filter 11

5. Conclusions and Recommendations 13

5.1 Conclusions 13

5.2 Recommendations 14

6. References 15

Appendix A. Engine Bench Specifications 17

Appendix B. Sensor Calibrations 27

List of Symbols, Abbreviations, and Acronyms 31

Distribution List 32

List of Figures

Fig. 1 In-cylinder pressure comparison at different combustion events 1
Fig. 2 Engine test bench 2
Fig. 3 Comparison of simple in-cylinder filters 4
Fig. 4 Biased heat-release rate using Savitzky-Golay filter 4
Fig. 5 Linear continuous-time filter order and phase response characteristics 5
Fig. 6 Comparison of linear continuous-time filters 6
Fig. 7 Magnitude response of linear time-continuous filters 8
Fig. 8 Magnitude response of linear time-continuous filters at a small field of view 9
Fig. 9 Raw and filtered in-cylinder pressure near combustion event 10
Fig. 10 Raw and filtered in-cylinder pressure near SOC 11
Fig. 11 Heat-release-rate calculation using different linear continuous-time filters 12
Fig. 12 Heat-release-rate calculation, including high-frequency pressure oscillation during combustion, using different filters 13
Fig. A-1 Kistler in-cylinder pressure sensor specification 18
Fig. A-2 Kistler fuel line pressure and temperature sensor/amplifier specification 19
Fig. A-3 Kistler fuel line pressure and temperature sensor/amplifier specification 20
Fig. A-4 Kistler optical encoder specification 21
Fig. A-5 Glow-plug specification 22
Fig. A-6 Kistler glow-plug adapter for Mercedes OM642 engine 23
Fig. A-7 Kistler glow-plug adapter for Mercedes OM642 engine 24
Fig. A-8 Re-Sol fuel, bench specification 26
Fig. A-9 Closed-loop cooling column specification 26
Fig. B-1 In-cylinder-pressure sensor calibrations 28
Fig. B-2 Static-pressure sensor calibrations 29
Fig. B-3 Thermocouple calibrations 30

1. Introduction

In-cylinder pressure data recorded during an internal combustion engine experiment is one of the most effective measurements to provide detailed information for combustion analysis. However, the use of raw in-cylinder pressure data is limited due to signal noise, and it is difficult to remove this noise while retaining characteristics of interest. A number of filters have been developed in the field of signal processing to remove unwanted noises and suppress interfering signals. There has been limited transition of these filters into the engine research community, where they perform well for normal engine operation. Either a simple moving-average-based filter or band-pass filter would remove signal noises for a normal engine combustion event that shows a gradual increase and decrease of in-cylinder pressure, shown as a red solid line in Fig. 1. However, when an abnormal combustion event occurs, the simple filters perform poorly near the transition point. Figure 1 shows an example of an extremely high-pressure rise cycle in a compression-ignition engine, shown as a black solid line, which cannot be filtered properly using simple filtering approaches.

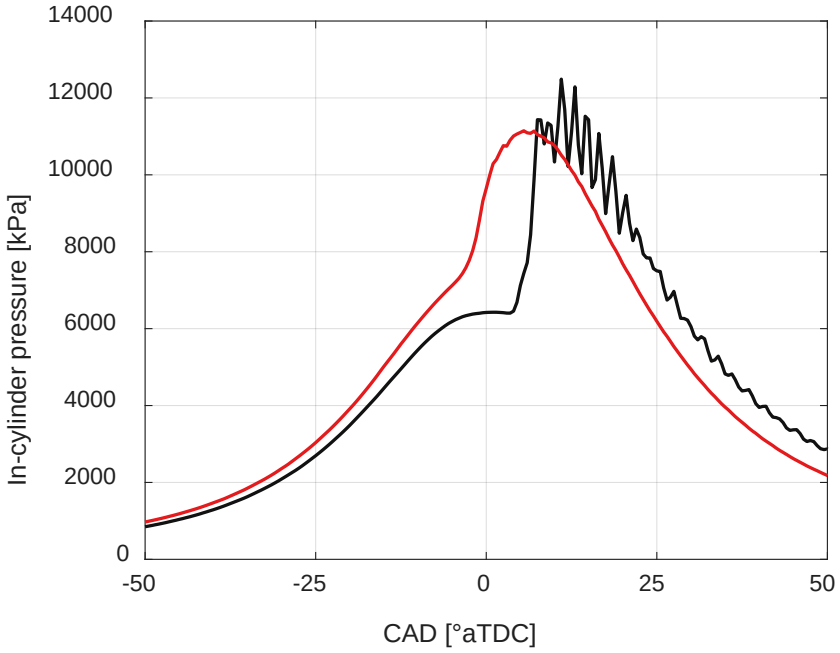

Fig. 1 In-cylinder pressure comparison at different combustion events

The objective of this study was to determine the optimal filter and relevant filter parameters that 1) remove signal noise recorded in a raw data and 2) maintain characteristics of in-cylinder pressure without any filter bias for both normal and abnormal combustion.

2. Experimental Setup

A 4-cylinder, turbocharged direct-injection aviation diesel engine was instrumented to acquire in-cylinder pressure data. Figure 2 shows the engine test bench. On the test stand, the engine is connected to an AC dynamometer that can operate up to 250 hp, with a maximum torque of 580 Nm and a maximum speed of 30,000 rpm. Engine crank angle was measured with a Kistler encoder (model no. 2614C11) with a resolution of 0.5° crank angle. In-cylinder pressure sensors were installed in the place of the glow plugs using off-the-shelf Kistler glow plug adapters (model no. 6544Q10). Detailed information on the glow plug and the glow plug adapter is shown in Appendix A. The calibrations of the major sensors can be found in Appendix B.

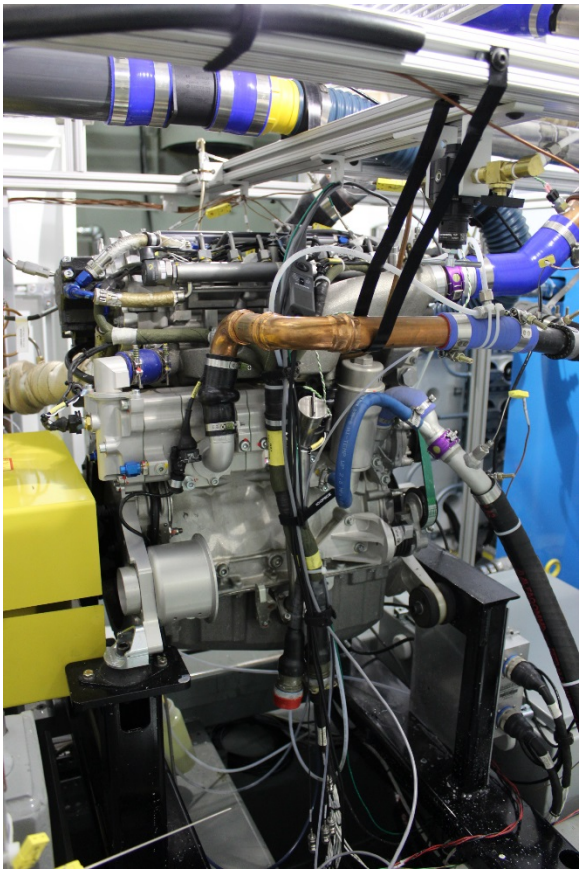

Fig. 2 Engine test bench

3. Filtering Approaches

This section discusses characteristics of differing filter types, limitation in filtering an erratic in-cylinder pressure, and optimal filter parameter design for engine research.

3.1 Simple Filters

A number of filters have been developed and recommended to fulfill different requirements of the analysis of engine experimental data. Simple smoothing filters such as a moving-average or median filter, are commonly used to reduce short-term fluctuations and highlight the long-term trend of the signal. The unweighted moving-average filter uses the simplest convolution operation and can serve as a low-pass filter. More-complex smoothing with a weighted moving-average can be achieved by using the Savitzky-Golay convolution coefficients, which are based on a least-squares fit of subsets of adjacent data points with a low-degree polynomial.

An engine test condition that showed high-pressure rise rate and high-frequency pressure oscillation was selected to demonstrate the capabilities and limitations of these simple filters. Two different data spans (5 and 10 points) were used for a moving-average filter, and 3rd-order polynomials were used for 1-D median filter. The built-in Matlab function sgolayfilt with a second-order polynomial and a frame length of 7 was used for a Savitzky-Golay filter. Figure 3 shows a comparison of all 4 filters against the original pressure data set. It is readily apparent that the Savitzky-Golay and the median filters exhibit excellent agreement with the in-cylinder pressure trace during compression stroke up until the start-of-combustion (SOC) around 4° aTDC (after top dead center). On the other hand, the moving-average filters showed deviations shortly before the initial pressure rise with higher-filtered pressure values. This is due to calculated average pressure in the window spreading the influence of the rapid pressure rise. As expected, a larger deviation was shown with the larger 10-point data span than the 5-point span. During the high-frequency pressure oscillation after the SOC, it is clear that the high-frequency signal noise was not effectively reduced or removed for any of the simple filters tested in Fig. 3. The median filter provided the worst performance among the tested filters, at some points even yielding the same value as the raw signal during the pressure oscillations after SOC. The Savitzky-Golay filter also showed relatively high oscillation compared with the moving-average filters. A tradeoff between accuracy near SOC and during pressure oscillations after SOC was found when simple filters were used. Figure 4 presents calculated heat-release and accumulative heat-release rates using the in-cylinder pressure signal filtered by Savitzky-Golay polynomials.

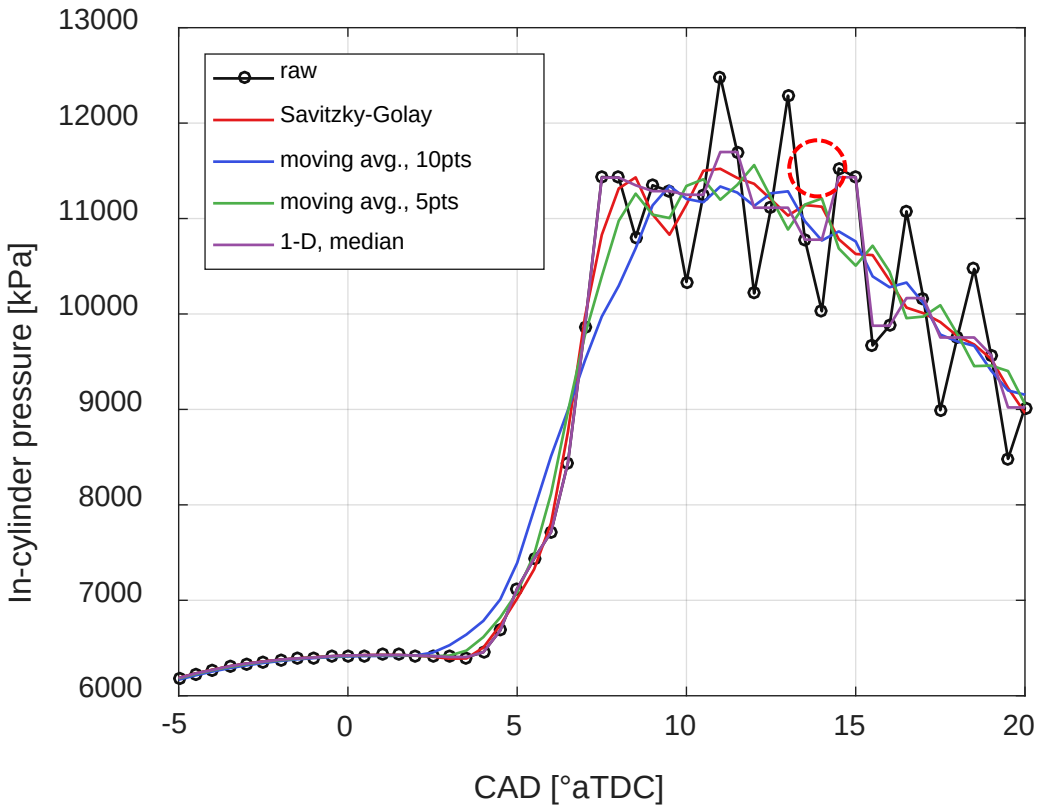

Fig. 3 Comparison of simple in-cylinder filters

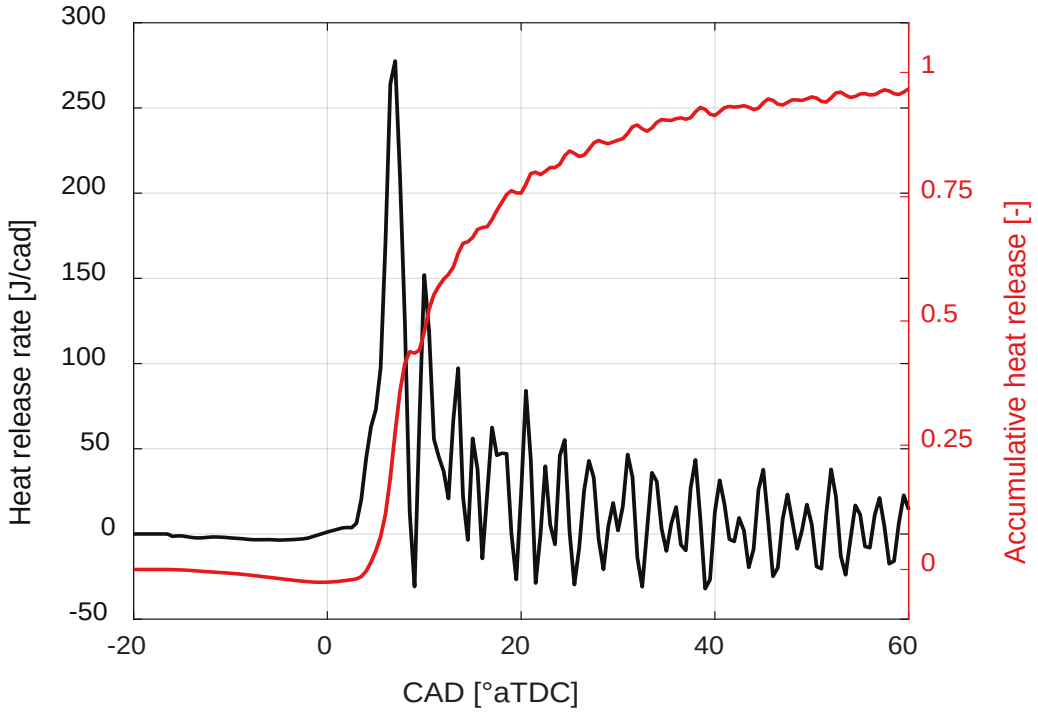

Fig. 4 Biased heat-release rate using Savitzky-Golay filter

Heat release rate was calculated using the first law of thermodynamics, as seen in Eq. 1, where γ is the time and temperature-dependent specific heat ratio, *V* is time-dependent combustion chamber volume, *P* is time-dependent in-cylinder combustion chamber pressure, and *Q* is energy added to the combustion chamber.[1]

$$\frac{dQ}{d\theta} = \frac{\gamma}{\gamma-1} P \frac{dV}{d\theta} + \frac{1}{\gamma-1} V \frac{dP}{d\theta} . \quad (1)$$

As shown in Eq. 2, γ was determined from a first-order polynomial equation, where *T* is the mean in-cylinder temperature obtained from the equation of state.[2]

$$\gamma = 1.392 - 7.35 \times 10^{-5} \times T . \quad (2)$$

Equation 1 shows hat the calculated rate of heat release is a strong function of both the pressure itself and the time derivative of the pressure data. The Savitzky-Golay filter removes noise effectively prior to the initial pressure rise, as seen in the calculated heat-release rate, which is close to zero. Additionally, the SOC can be determined with the least uncertainty using this set of filtered in-cylinder pressure data. However, the inefficiency of the Savitzky-Golay filter during the pressure oscillation phase is transferred to the heat-release calculation, and the oscillations in calculated heat-release rate can be seen in Fig. 4. During the oscillation, negative values of the heat-release rates are seen, which is not physically possible and mostly due to filter bias.

3.2 Linear Continuous-Time Filter

3.2.1 Filter Comparison

Various linear continuous-time filters, which operate in the frequency domain, were investigated to compare filter response characteristics and noise reduction performance. Figure 5 illustrates the basic characteristics of the filters with regard to filter order and phase response.[3] No single filter performs perfectly for all possible experimental setups; therefore, a filter should be selected with care to efficiently filter the raw signal. In this report, Butterworth, Chebyshev, and elliptic filters, which are the most widely used linear continuous-time filters, are compared.

Fig. 5 Linear continuous-time filter order and phase response characteristics[3]

Figure 6 presents the magnitude response of the Butterworth, Chebyshev Type 1 and 2, and elliptic filters with respect to a signal frequency. The Butterworth is a well-known and widely used filter that is often referred to as a maximally flat magnitude filter. It was designed not only to remove certain frequencies, but also to maintain a uniform sensitivity for the frequencies of interest. To allow a uniform sensitivity for both passband and stopband without any ripples, the Butterworth filter shows the slowest roll-off of the signal magnitude decrease and widest frequency range compared with the other filters shown in Fig. 6. A 4th-order polynomial was used for the Butterworth filter, and the slope of the filter can be adjusted by changing the order of polynomial. Higher order will make the Butterworth filter sharper at the cutoff frequency; however, the magnitude response value of any order will be the same at the cutoff frequency, approximately at 0.7.

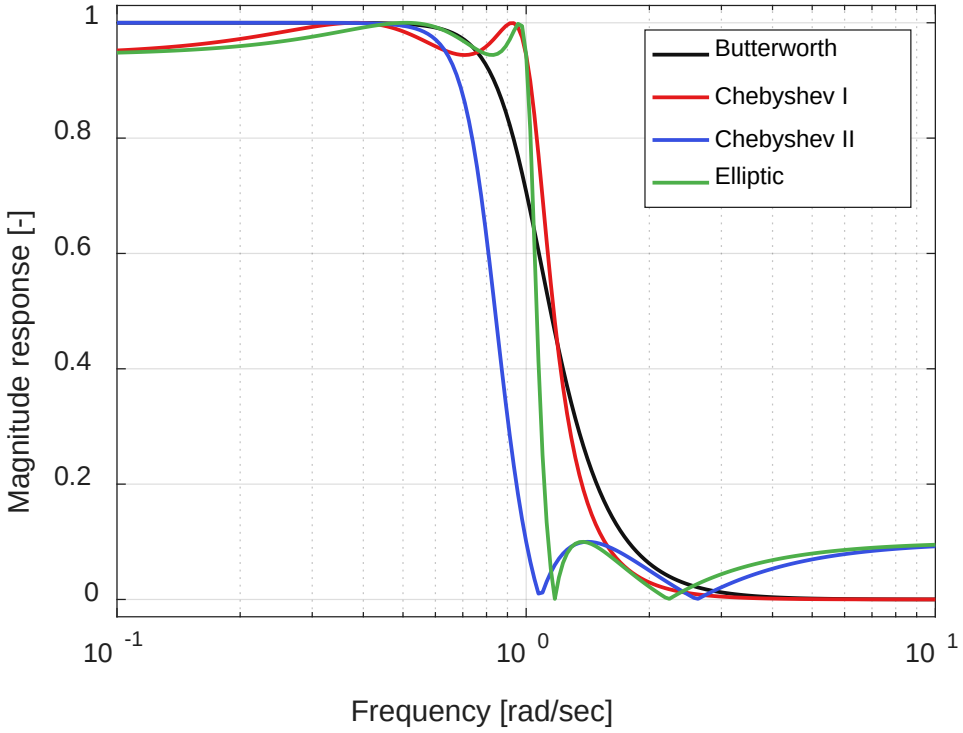

Fig. 6 Comparison of linear continuous-time filters

The Chebyshev filter is known as the best approximation to the ideal step response with steeper roll-off at the cutoff frequency by allowing oscillations in the passband. Type 1 has ripples in the passband, while Type 2 has ripples in the stopband. The elliptic filter has ripples in both passband and stopband with the steepest roll-off of all the filters. Figure 6 shows the filter magnitude response of a 4th-order Chebyshev Type 1 with a 0.5-dB ripple in passband and a Type 2 with a 20-dB ripple in stopband and an elliptic filter with the same order and ripple factor. The elliptic filter showed the steepest magnitude response at the cutoff frequency;

however, ripples in the both stopband and passband can cause bias. As the ripples in the passband approaches zero, the elliptic filter becomes a Type 1 Chebyshev filter, and reduced ripples in the stopband becomes similar to the Type 2 filter. A Butterworth filter is the extreme case of a Chebyshev filter without any oscillations over the whole bandwidth.

3.2.2 Filter Optimization

For the purpose of combustion analysis, a stable low-pass-filtered in-cylinder pressure is very critical. To determine as accurately as possible the metrics of an erratic combustion event (e.g., pressure rise rate and knock intensity), the least-biased bandpass-filtered data are required. To avoid filter bias and over-filtering issues, flat magnitude responses at low frequency (passband) are preferred; therefore, Butterworth and Chebyshev Type 1 filters with ripples at the passband were compared with different parameters.

Figure 7 shows magnitude responses of filters with different cutoff frequencies, order of polynomials, and ripple allowances. The Butterworth filters were compared with 2 different cutoff frequencies, 4 and 5 kHz. A normalized cutoff frequency of 4 kHz (0.1852 π×rad/sample) is marked in the figure to visually confirm filter response at the cutoff frequency. Figure 7 shows that the magnitude response of the Butterworth filters with a 4-kHz cutoff frequency starts decreasing at the normalized frequency of 0.14 π×rad/sample, which is equivalent to a 3-kHz in-frequency domain. Even with a 5-kHz cutoff frequency, the Butterworth filter showed a magnitude response of 0.96 [-] at the normalized frequency due to the slow roll-off characteristics. The Butterworth filter has an advantage of maximum flat magnitude response; however, as a tradeoff, the filter showed less sensitivity responding to the desired cutoff frequency.

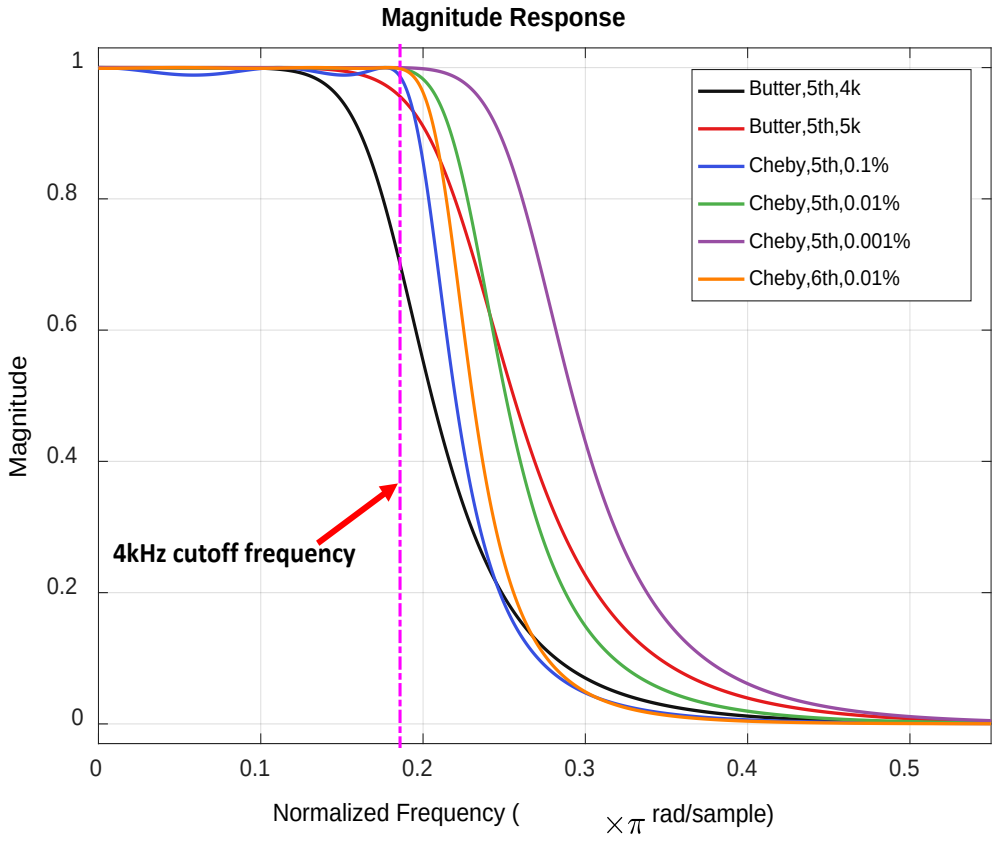

Fig. 7 Magnitude response of linear time-continuous filters

The magnitude response of the Chebyshev Type 1 filter with a different order of polynomials, and therefore acceptable levels of oscillation, are presented in Fig. 7. Compared with the Butterworth filters, the Chebyshev filters showed relatively faster roll-off between passband and stopband. As the level of acceptable oscillation increased, magnitude response decreased slowly, or the same level of magnitude was achieved at higher normalized frequency. The higher-order polynomial showed slightly steeper magnitude response. Every tested Chebyshev filter showed an initial decrease of the magnitude response very close to the targeted cutoff frequency.

Figure 8 presents the magnitude response of different filters discussed in Fig. 7 with a smaller field of view at the passband. Ripples allowed in the passband for Chebyshev filters are clearly shown. The amount of allowed oscillation is shown in decibels and not with the absolute value of magnitude. For any orders of polynomial and allowed ripples, the Chebyshev filter showed good response of decreased magnitude at the targeted cutoff frequency. When compared with different magnitudes of acceptable oscillation at the same order of polynomials, the location of the ripples were the same with only differences in the amplitude of the ripples.

A higher order of polynomial at the same allowed ripples shows a slightly steeper magnitude response around the targeted cutoff frequency. In the passband frequency range, the 6th-order polynomial showed one more ripple than the 5th-order polynomial, which resulted in less than unity of the magnitude response at the lowest frequency range. Odd numbers of polynomial orders are preferred for the optimized Chebyshev filter parameters, with magnitude response close to unity at the lowest frequency.

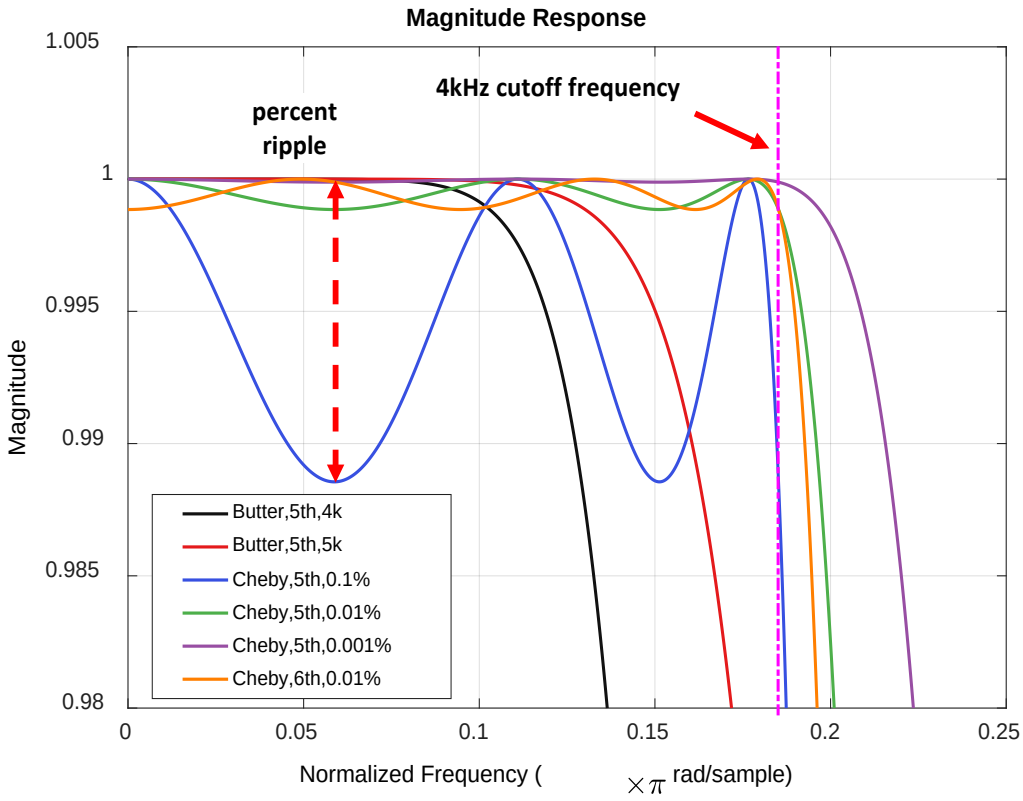

Fig. 8 Magnitude response of linear time-continuous filters at a small field of view

4. Results and Discussion

Linear time-continuous filters discussed in the previous section were applied to in-cylinder pressure data to compare filter performances.

4.1 Filtered In-Cylinder Pressure

Figure 9 presents raw and filtered in-cylinder pressure signals at a long ignition delay condition to evaluate filter performance. A Butterworth filter with a 5th-order polynomial using a 4-kHz cutoff frequency and a Savitzky-Golay filter with second-order polynomial using a frame length of 7 were used as low-pass filters to calculate filtered in-cylinder pressure traces. As discussed in the previous section,

only a 5th-order polynomial was used for Chebyshev filter. The filtered in-cylinder pressure using the Savitzky-Golay filter and the Chebyshev with 0.001%-allowed ripples showed good agreement with the raw in-cylinder pressure data around SOC timing (from top dead center [TDC] to 3° aTDC), while pressure oscillation are observed after the initial pressure rise (after 5° aTDC). Other filters, including the Butterworth and the Chebyshev with a larger amplitude of ripples allowed, showed deviations at SOC timing and less oscillations after the initial pressure rise.

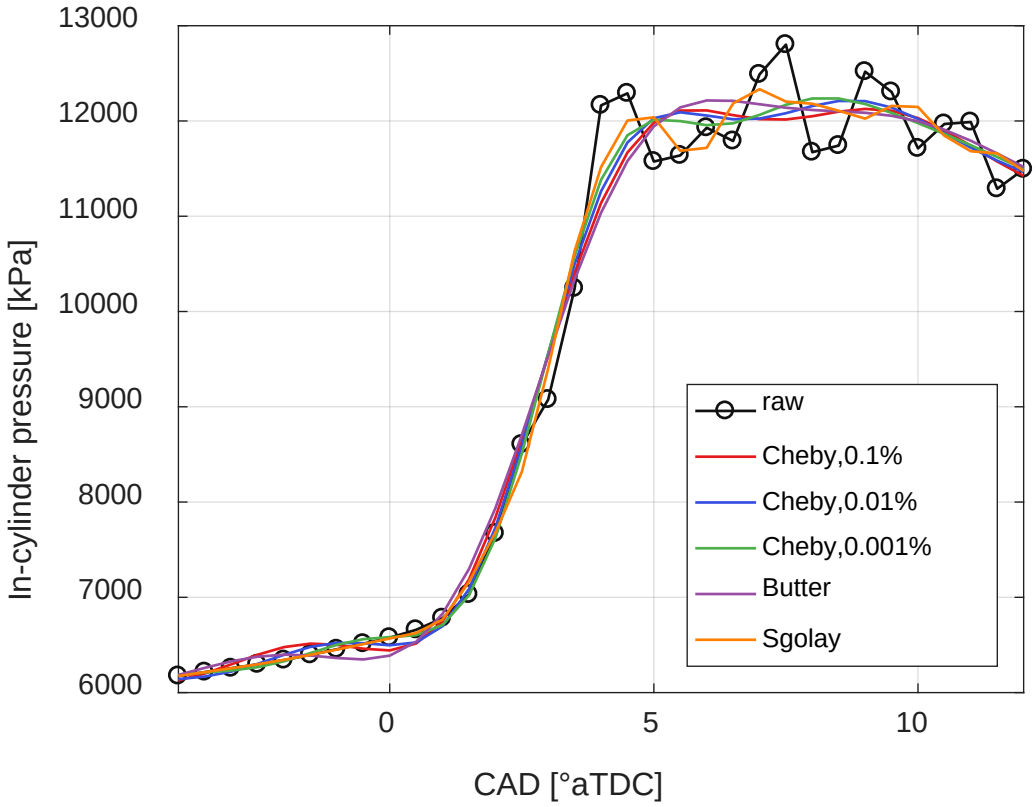

Fig. 9 Raw and filtered in-cylinder pressure near combustion event

Figure 10 presents the same data as seen in Fig. 9 but at a smaller field of view to focus filtered in-cylinder pressure data at SOC timing. Over-filtered in-cylinder pressure as pressure fluctuations ahead of SOC were shown with the Butterworth and Chebyshev filters. The Butterworth filter showed the highest deviations, about 150 kPa, compared with the raw data at a few crank-angle degrees ahead of SOC timing. Any biases at SOC timing will significantly impact determining SOC and initial heat-release results. The Chebyshev filter with 0.001%-allowed ripples showed reasonable deviations with a less than 50-kPa difference around SOC timing.

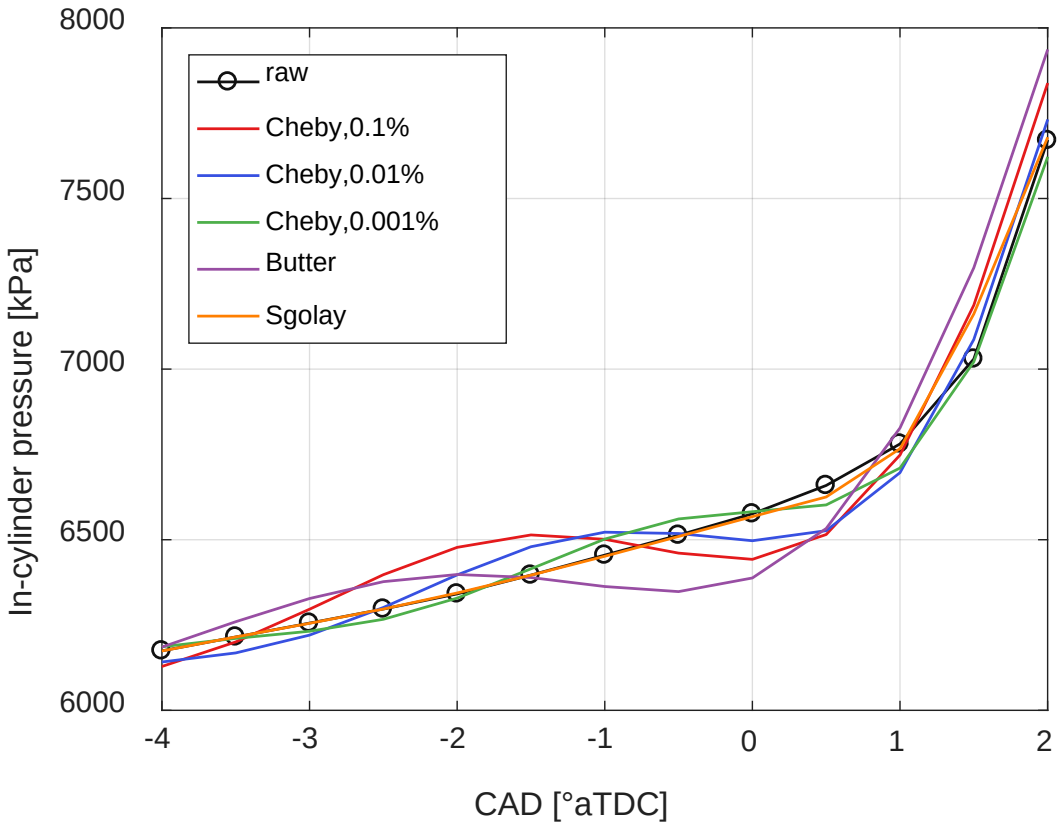

Fig. 10 Raw and filtered in-cylinder pressure near SOC

4.2 Heat-Release-Rate Results using the New Filter

Figure 11 presents calculated heat-release-rate results using different linear continuous-time filters. Results calculated using the Savitzky-Golay-filtered in-cylinder pressure data clearly showed the timing of an initial combustion event, while other filters showed fluctuations before SOC. These fluctuations are not physically possible and are purely due to over-filtering bias in the in-cylinder pressure trace. The Chebyshev filter with 0.001%-allowed ripples showed fewer fluctuations than other filters, and the value of the peak heat-release rate was reasonably well-matched with the Savitzky-Golay filter. After the initial premixed combustion, a reasonable trace of heat-release rate with less oscillation and no negative values were shown with the Chebyshev and Butterworth filters. The Butterworth filter showed the least fluctuation of all the filters; however, in-cylinder pressure data and heat-release-rate calculation at SOC could be significantly biased due to over-filtering.

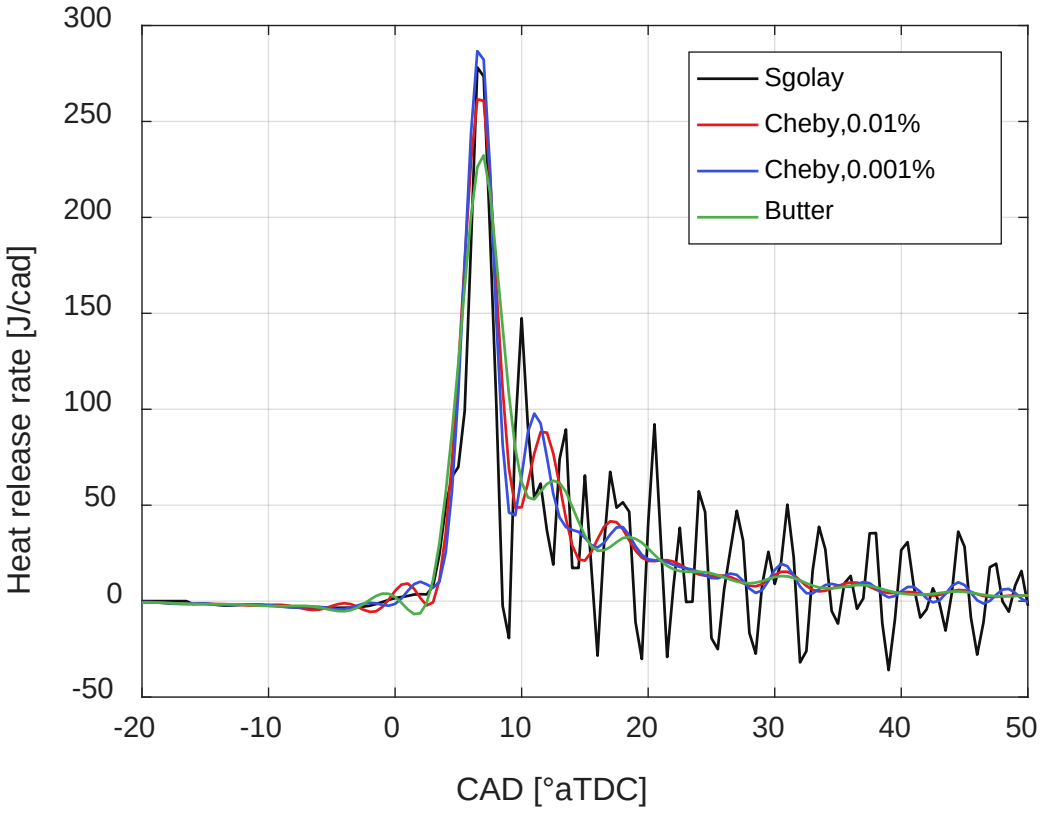

Fig. 11 Heat-release-rate calculation using different linear continuous-time filters

Figure 12 presents calculated heat-release rate that includes high-frequency pressure oscillation during combustion. The pressure oscillations that were captured by the Savitzky-Golay filter were shown as high-frequency oscillations in the heat-release calculation. With the use of any linear continuous-time filters investigated in this report, the nonphysical heat-release-rate oscillations were reduced. A clearer separation between premixed and mixing-controlled combustion can be achieved with either Chebyshev or Butterworth filters.

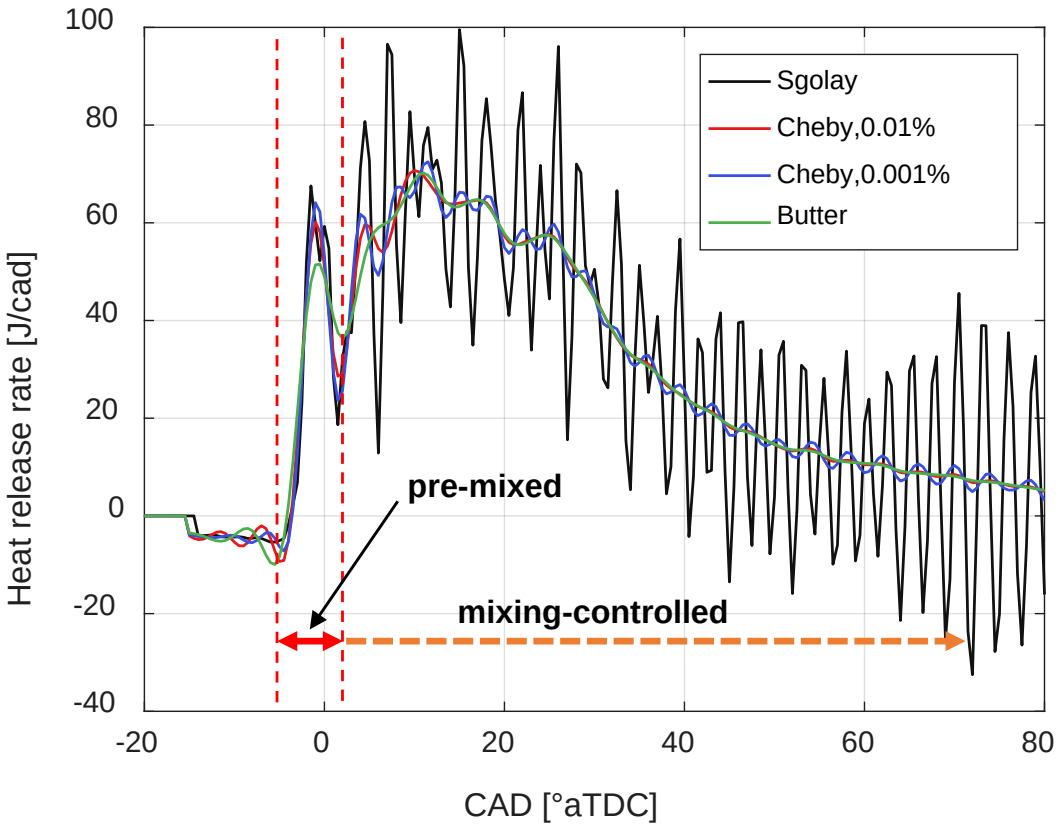

Fig. 12 Heat-release-rate calculation, including high-frequency pressure oscillation during combustion, using different filters

5. Conclusions and Recommendations

The in-cylinder pressure data from engine research requires proper filtering for combustion analysis, especially with the existence of erratic combustion events. The objective of this research was to investigate linear continuous-time filter characteristics and their performance filtering engine in-cylinder pressure data to remove noise in the raw data without causing any filter bias. To achieve this goal, a number of filters were tested, and the Chebyshev Type 1 filter with optimal parameters was determined to be an optimal filter for analysis of an aviation diesel engine in-cylinder data.

5.1 Conclusions

A relatively simple filter, based on a moving-average calculation, cannot sufficiently remove signal noise in the raw data. Linear continuous-time filters were compared to determine the optimal parameters that filters engine in-cylinder data for both normal and erratic combustion with minimal filter biases. The Butterworth filter provides stable filtered signal with its maximally flat magnitude response but

under-performs with sudden pressure increase. Filter response to a cutoff frequency was low due to a slow roll-off characteristic of the Butterworth filter. The Chebyshev filter showed a good response of decreased magnitude response at the targeted cutoff frequency for any order of polynomials and allowed ripples. The Chebyshev Type 1 filter with 5th-order polynomial and 0.001%-allowed ripples showed good agreement with experimental data near SOC timing and significantly lower signal oscillations than the Savitzky-Golay filter.

5.2 Recommendations

From the investigation of linear continuous-time filters' characteristics and performance, it was found that the filter should be selected with care to ensure noise removal and maintaining the accuracy of in-cylinder pressure trace. The following recommendations are made for potential future use of in-cylinder filters:

- The Butterworth filter calculates filtered pressure with reasonable accuracy for normal combustion. In the case of an erratic combustion, the Butterworth filter resulted biases, especially at the start of combustion with a high-pressure rise.
- The Chebyshev Type 1 filter performed well, filtering both normal and erratic combustion in-cylinder pressure data. An odd-number polynomial order is suggested to ensure flat response at the lowest frequency range.
- An energy spectral density analysis of the engine system is required to determine the natural frequency of the engine block to effectively remove unwanted frequency ranges.

6. References

1. Heywood JB. Internal combustion engine fundamentals. New York (NY): McGraw-Hill; 1988.
2. Gatowski J, Balles E, Chun K, Nelson F, Ekchian J, Heywood J. Heat release analysis of engine pressure data. Warrendale (PA): Society of Automotive Engineeers; 1984. SAE Technical Paper No.: 841359.
3. Orfanidis S. Lecture notes on elliptic filter design. New Brunswick (NJ): Department of Electrical and Computer Engineering, Rutgers University; 2006.

INTENTIONALLY LEFT BLANK.

Appendix A. Engine Bench Specifications

Kistler In-cylinder Pressure Sensor		
Model Number	[]	6058A
Range	[bar]	0 ... 250
Overload	[bar]	300
Sensitivity	[pC/bar]	-17
Natural frequency, nominal	[kHz]	160
Linearity	[%FSO]	0.3
Acceleration sensitivity	[bar/g]	<0.0005
Operating temperature range	[°C]	-50 ... 400
Sensitivity shift		
200±50°C	[%]	±0.5
23 ... 350°C	[%]	±2
Short term drift (thermal shock) (at 1 500 1/min, pmi = 9 bar)		
|Δp| (Short therm drift)	[bar]	<0.5
|Δpmi|	[%]	<2
|Δpmax|	[%]	<1
Insulation resistance at 23 °C	[Ohm]	>10^13
Shock resistance	[g]	2000
Capacitance, without cable	[pF]	5
Weight with cable	[gram]	30
Tightening torque	[Nm]	1.2
Connector, ceramic insulator	[]	M3×0.35

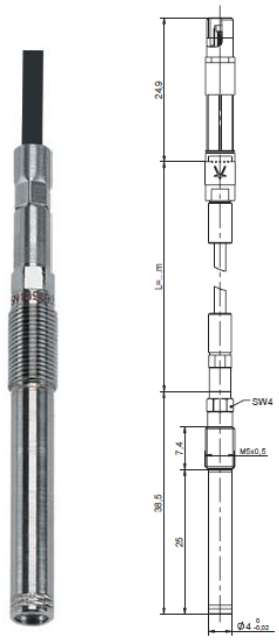

Fig. A-1 Kistler in-cylinder pressure sensor specification

Kistler Fuel Line Pressure and Temperature Sensor / Amplifier		
Model Number	[]	4067C3000 / 4618A2
Range	[bar]	0 ... 3000
Overload	[bar]	3500
Threshold	[mbar]	200
Sensitivity (± 0.5 % at 25°C)	[mV/bar]	5
Natural frequency (sensor)	[kHz]	>100
Rise time (5-95 %)	[µs]	<10
Output signal, pressure	[V]	0 ... 10
Output signal, temperature	[mV/K]	10
Output resistance	[Ohm]	10
Supply (amplifier)	[VDC]	18 ... 30
Zero setting (at 25°C, 1 bara)	[mV]	<±100
Linearity and hysteresis	[% FSO]	<±1
Thermal shift (20 ... 120 °C) of		
Zero	[% FSO]	<±2
Sensitivity	[%]	<±2
Operating temperature range		
Sensor	[°C]	10 ... 120
Amplifier	[°C]	0 ... 70
Minimum/maximum temperature (sensor)	[°C]	–40/140
Acceleration sensitivity	[mbar/g]	
Vibration resistance	[g]	1000
Tightening torque	[Nm]	15
Degree of protection	[]	IP 65
Service life (guideline)	[cycles]	>10^7

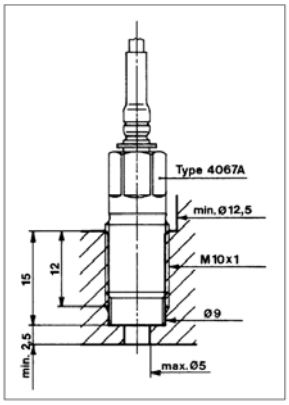

Fig. A-2 Kistler fuel line pressure and temperature sensor/amplifier specification

Kistler Manifold Air Pressure Piezoresistive Sensor		
Model Number	[]	4045A5
Range	[bar]	0 ... 5
Overload	[bar]	12.5
Threshold	[mbar]	<2.5
Burst pressure	[bar]	12.5
Sensitivity (± 0.5 % at 25°C)	[mV/bar]	100
Natural frequency (sensor)	[kHz]	>30
Full scale output	[mV/bar]	500
Constant current excitation	[mA]	<10
Calibration current	[mA]	2 ... 5
Input/output impedance	[kOhm]	3 (nominal)
Zero measured output	[mV/bar]	<±20
Linearity	[%FSO]	<±0.3
Hysteresis	[%FSO]	<0.1
Repeatability	[%FSO]	<0.2
Stability of sensitivity		<0.2
Stability of zero	[%FSO]	<0.1
Thermal zero shift	[%FSO]	<±0.5
Thermal sensitivity shift	[V]	<±1
Operating temperature range	[°C]	20 ... 120
Minimum/maximum temperature	[°C]	0 / 140
Acceleration error	[bar/g]	<3×10^(-4)
Shock resistance	[g]	1000
Volume change	[mm3]	<0.2
Insulation Resistance	[megaOhm]	>100
Material (head and diaphragm)	[]	18/8 steel
Material (body with threads)	[]	Armco 17-4 PH
Tightening torque (with Delrin plastic gasket)	[Nm]	3 ... 5
Socket for plug	[]	Fisher Type SE 103A054

Fig. A-3 Kistler fuel line pressure and temperature sensor/amplifier specification

Kistler Optical Encoder		
Model Number	[]	2614C11
Crank angle signal	[°]	720x0.5
Speed range	[1/min]	0 … 12 000
Temperature rang	[°C]	–40 … 85
Mechanical Interface/Mounting diameter	[mm]	60
(mounting compatibility to Type 2614B1)		
Electrical connection		cable with plug l = 2 m
Weight	[g]	340
Control & Indication LED's	–	Power
	–	Rotation cw/ccw
	–	Trigger
	–	Synchronization
Output signal to Indicating System	–	LVDS-Signal
	–	TTL-Signal
Power supply	[VDC]	5 ... 30
Temperature range	[°C]	–30 ... 70
Dimensions	[mm]	108x74x36
Weight	[g]	290

Fig. A-4 Kistler optical encoder specification

BERU

Article Details 06.01.2012

Brand	BERU
Article Number	0100266011
Description	Glow Plug
EAN	40 14427 08190 6
Packing Unit	1
Quantity per Packing Unit	1
Trade Number	GE 105
Supersedes	0100266007

Properties

Voltage [V] 4,4
After-glow capable
Pencil-type Glow Plug
Spanner Size 8 mm
Thread Size M 8x1
Overall Length [mm] 148,5
Fitting Depth [mm] 27
Cone Pitch 93°
Port Type Ø 4 mm
Failure Moment [Nm] 20
Tightening Torque [Nm] 10

BERU

Information/Safety Notes

Installation Information:

- Cover glow plug thread and -shaft with mounting grease, (GKF 01 - Order No. 0 890 300 034), before fitting to enable easier removal and prevent corrosion.

OE Numbers

Brand	Number
JEEP	0517 5756 AA
MERCEDES-BENZ	001 159 50 01
	A 001 159 50 01

Fig. A-5 Glow-plug specification

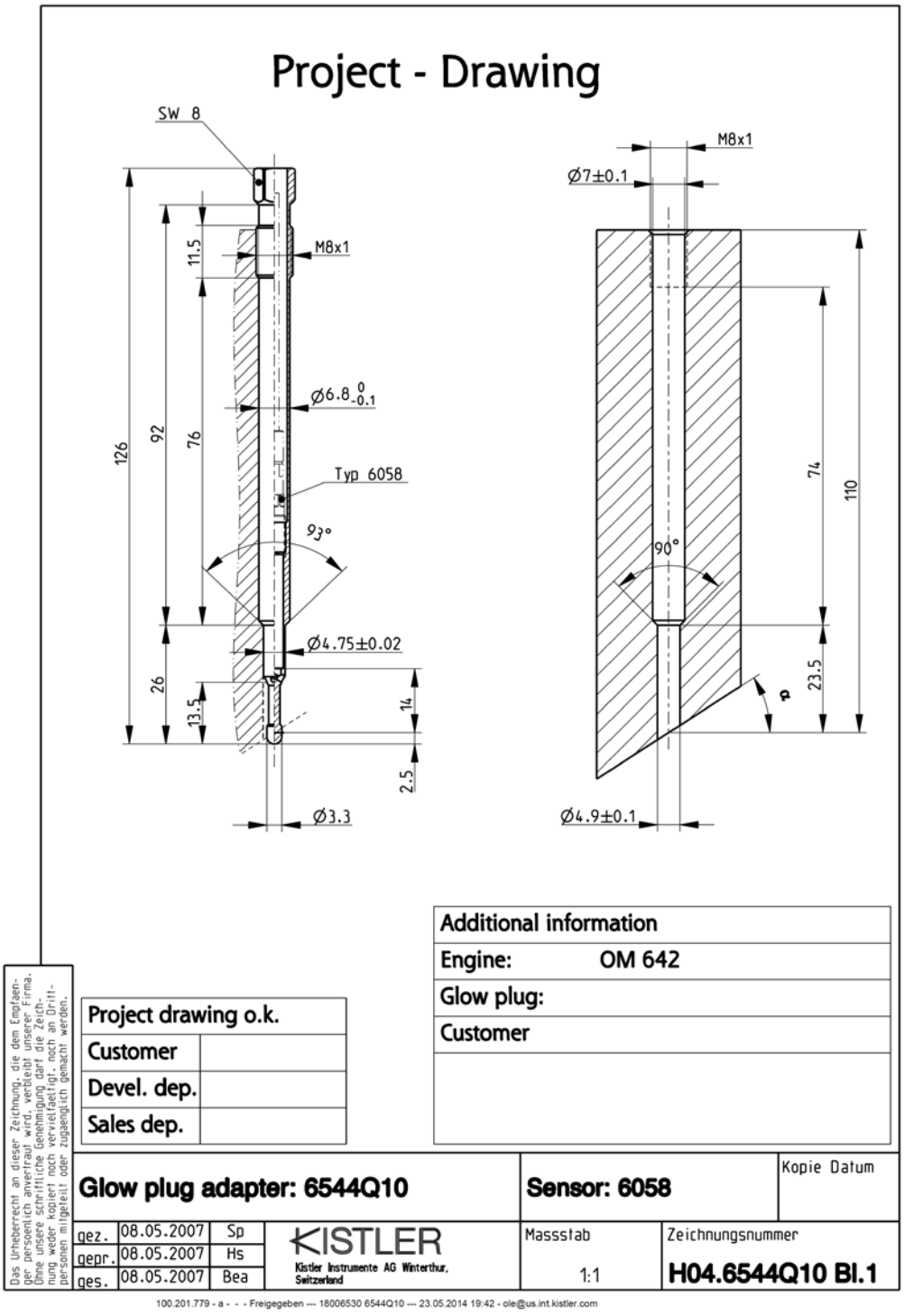

Fig. A-6 Kistler glow-plug adapter for Mercedes OM642 engine

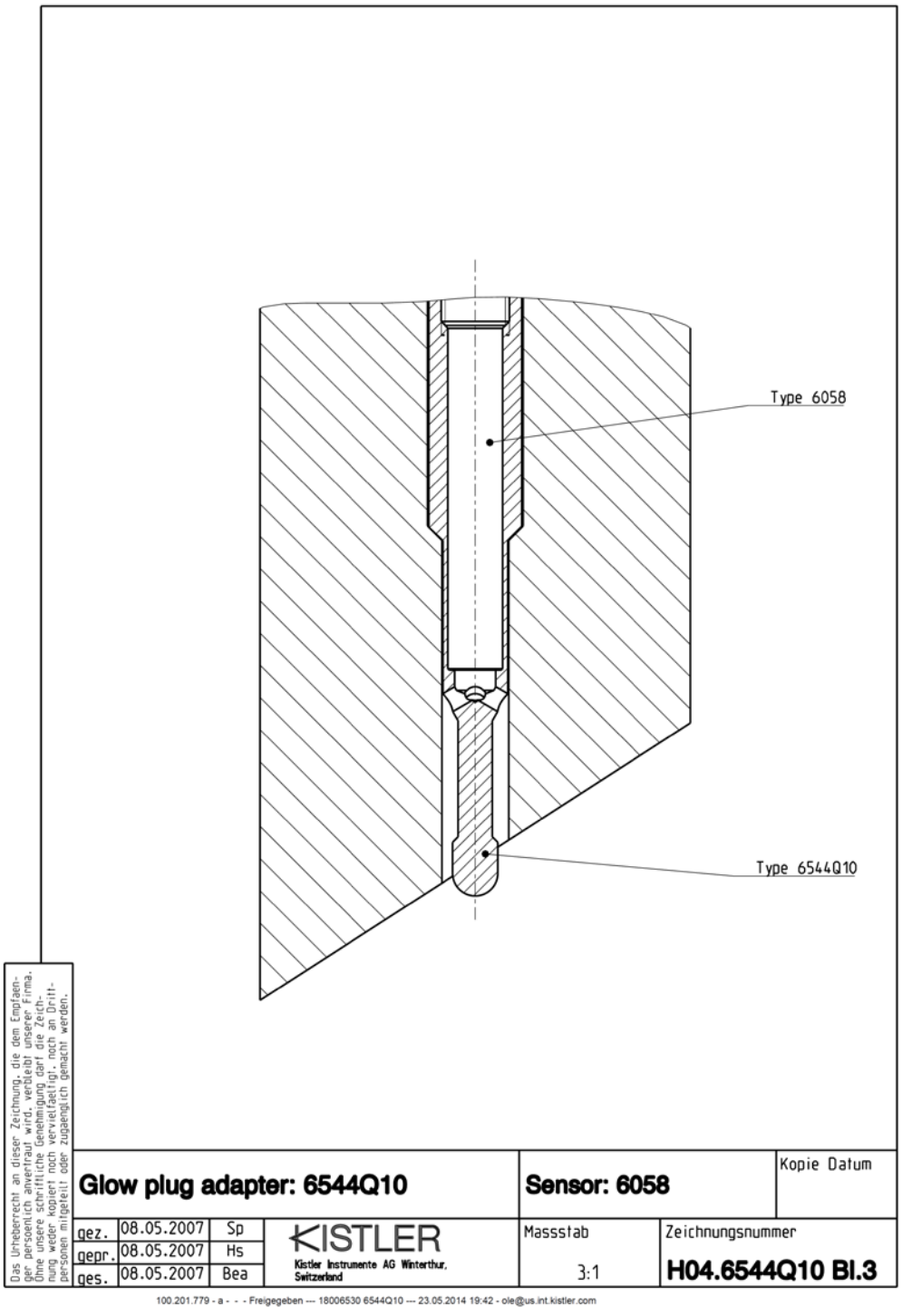

Fig. A-7 Kistler glow-plug adapter for Mercedes OM642 engine

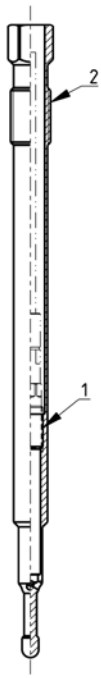

Mounting Instruction

1. Firstly mount the sensor into the adapter.
   Mounting torque: Type 6058: 1,2Nm

2. Mount the adapter (including the sensor) into the cylinderhead, applying the same mounting torque as for the original glow plug. Standard value:
   Mounting torque for glow plugs: M8: 8...12 Nm
   M10: 10...15 Nm
   M12: 15...20 Nm

Technical Data

Sensor Type 6058

- Sensitivity	[pC/bar]	-16
- Measuring range	[bar]	0...250
- Operating temperature range	[°C]	-50...350

Accessories for Sensor Type 6058

- Connecting cable Viton M3x0,35 pos.	Type 1989A411
- Mountig key	Type 1300A14
- Torque wrench 1...6Nm	Type 1300A17

Resonance of Pipe Oscillation

- Calculated 1st resonance frequency: (with Bergh & Tijdeman approach)	>11,0 kHz
- Glow plug tip volume (below sealing face):	252,0 mm³
- Tip volume with original glow plug:	236,0 mm³

Glow plug adapter: 6544Q10 | **Sensor: 6058** | Kopie Datum

gez.	08.05.2007	Sp	KISTLER Kistler Instrumente AG Winterthur, Switzerland	Massstab 1:1	Zeichnungsnummer **H04.6544Q10 Bl.2**
gepr.	08.05.2007	Hs			
ges.	08.05.2007	Bea			

100.201.779 - a - - - Freigegeben --- 18006530 6544Q10 --- 23.05.2014 19:42 - ole@us.int.kistler.com

Fig. A-7 Kistler glow-plug adapter for Mercedes OM642 engine (continued)

Re-Sol Fuel Bench	
Model	RS905C
Fuel Type	JP-8, Jet fuels, diesel, synthetic JP-8, bio fuels
Flow Measurement Range	0.1 to 15g/s
Engine Supply Pressure	120 PSI
Pressure Control Stability	+/- 0.75 PSI
Temperature Accuracy	Better than +/- 0.5°C
Temperature Control Range	30°C to 50°C
Density Range	0.6 to 0.9 g/cc
Fuel Capacity	Two 6 gallon reservoirs
Cooling Capacity	6 kW
Cooling water flow	4 gpm with 20 psi differential
Shop Air Supply Pressure	Minimum 40 PSI
Power	120 VAC, Single-Phase, 4.8 FLA, 60 Hz

Fig. A-8 Re-Sol fuel, bench specification

PTI Closed-Loop Cooling System			
Category	**Description**	**Unit**	**Value**
System	Model	[]	CLC-300
	Serial number	[]	63844
	Max power	[hp]	300
	Estimated weight	[lbs]	600
Engine	Max inlet temp.	[°F]	230
	Max pressure	[psi]	15
Water	Max inlet temp	[°F]	85
	Pressure pange	[psi]	30-65
	Min flow / 100 hp	[gpm]	7
Power	Power requirement	[VAC]	120
	Max current	[A]	15

Fig. A-9 Closed-loop cooling column specification

Appendix B. Sensor Calibrations

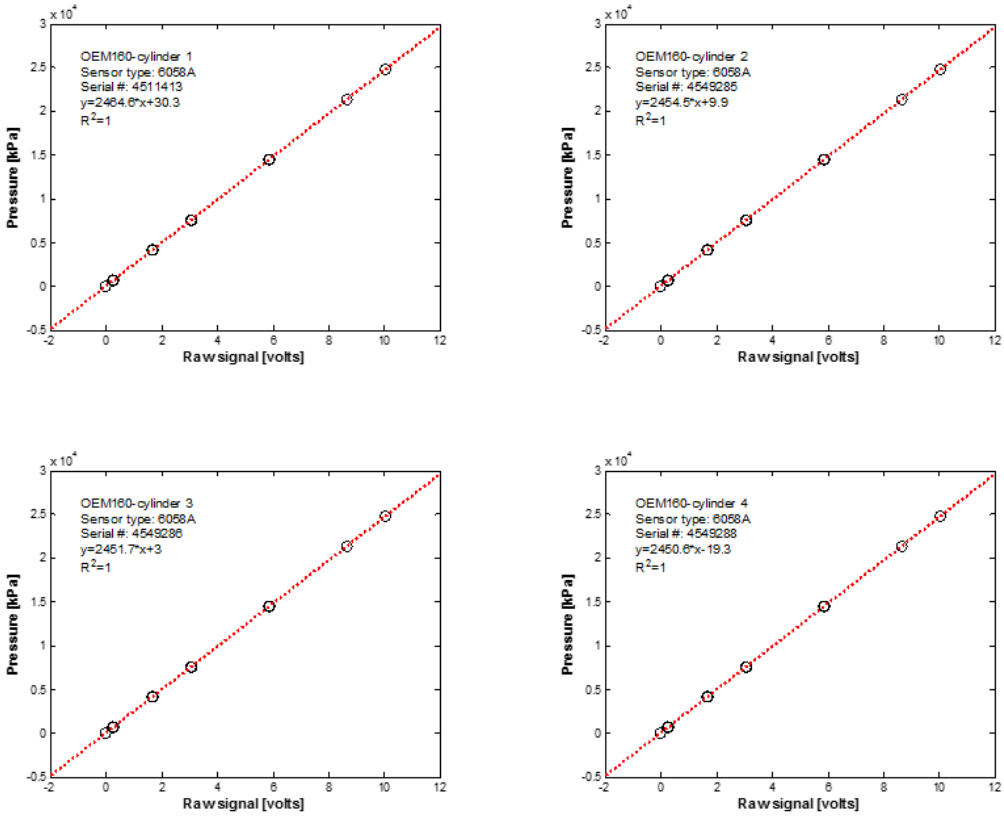

Fig. B-1 In-cylinder-pressure sensor calibrations

A1: Oil pressure to PTI P1 (0-250PSI)		
Nominal (PSI)	Fluke (PSIG)	PTI (PSIG)
0	0.1	2.1
50	48.5	49.6
100	97.5	98.8
150	147.3	149.0
200	199.0	201.0

B1: Coolant from engine to cooling column (Omega PX319-200AI, 0-200PSIA, 4-20mA)		
Nominal (PSI)	Fluke (PSIG)	NI Dac (mA)
0	0.1	5.2
50	48.3	9.0
100	98.3	13.0
150	148.3	17.1
200	186.6	20.1

A2: Intake pressure to PTI P2 (0-250PSI)		
Nominal (PSI)	Fluke (PSIG)	PTI (PSIG)
0	0.1	-0.1
50	48.3	48.2
100	97.6	97.7
150	147.9	148.0
200	199.0	199.0

B2: Exhaust manifold pressure (Omega PX319-200AI, 0-200PSIA, 4-20mA)		
Nominal (PSI)	Fluke (PSIG)	NI Dac (mA)
0	0.1	5.2
50	47.6	9.0
100	97.9	13.0
150	147.2	17.0
200	185.6	20.1

A3: Exhaust pressure to PTI P3 (0-50PSI)		
Nominal (PSI)	Fluke (PSIG)	PTI (PSIG)
0	0.1	0.0
10	8.1	8.1
20	17.9	17.9
30	28.3	28.4
40	38.2	38.3
50	47.1	47.1

B3: Air from surge tank to compressor (Omega PX319-200AI, 0-200PSIA, 4-20mA)		
Nominal (PSI)	Fluke (PSIG)	NI Dac (mA)
0	0.2	5.2
50	49.1	9.1
100	97.1	12.9
150	146.4	16.9
200	184.8	20.0

A4: Spare PTI P4 (0-5PSI)		
Nominal (PSI)	Fluke (PSIG)	PTI (PSIG)
0	0.000	0.9
1	0.640	1.5
2	2.008	2.9
3	3.278	4.2
5	4.917	5.8

B4: Coolant from cooling column to engine (Omega PX319-200AI, 0-200PSIA, 4-20mA)		
Nominal (PSI)	Fluke (PSIG)	NI Dac (mA)
0	0.1	5.2
50	47.5	9.0
100	97.1	12.9
150	146.2	16.9
200	184.8	20.0

A5: Spare (Omega PX319-200AI, 0-200PSIA, 4-20mA)		
Nominal (PSI)	Fluke (PSIG)	NI Dac (mA)
0	0.0	5.2
50	45.1	8.8
100	96.0	12.9
150	146.0	16.9
200	182.0	19.7

B5: Exhaust surge tank (Omega PX319-30AI, 0-30PSIA, 4-20mA)		
Nominal (PSI)	Fluke (PSIG)	NI Dac (mA)
-15	-14.738	4.0
-8	-8.078	7.6
0	0.100	11.9
8	6.600	15.5
15	14.200	19.5

New sensor for exhaust duct (Omega 26-32"Hg, 4-20mA)		
Nominal (PSI)	Fluke (PSIG)	NI Dac (mA)
1.0	0.978	20.3
0.5	0.505	17.8
0.0	0.000	15.1
-2.0	-1.711	5.8
-3.0	-2.155	3.2
-4.0	-2.627	2.0

Fig. B-2 Static-pressure sensor calibrations

Ref	PTI Module	Thermocouple	TC name	Sourced Temperature on Calibrator [°C]			
				-200.0	193.0	586.0	979.0
				Reading [°C]			
1	1	1	Cyl 1 exh	-198.3	193.9	586.7	979.4
2	1	2	Cyl 2 exh	-198.3	193.9	586.7	979.4
3	1	3	Cyl 3 exh	-198.3	193.9	586.7	979.4
4	1	4	Cyl 4 exh	-198.3	193.9	586.7	979.4
5	1	5	Exh Mnfld	-198.3	193.9	586.7	979.4
6	1	6	Oil	-198.3	193.3	586.7	979.4
7	1	7	Exh Pipe	-198.3	193.3	586.7	979.4
8	1	8	Intake Pipe	-198.3	193.3	586.7	979.4
9	2	1	Intake Mnfld	-198.3	193.3	586.7	979.4
10	2	2	Coolant Supply	-198.3	193.3	586.7	979.4
11	2	3	Coolant Return	-198.9	193.3	586.7	979.4
12	2	4	Exh Surge Tank	-198.9	193.3	586.7	979.4
13	2	5	Ambient	-198.3	193.3	586.7	979.4
14	2	6	Unused	-198.3	193.3	586.7	979.4
15	2	7	Unused	-198.3	193.3	586.7	979.4
16	2	8	Unused	-198.3	193.3	586.7	979.4

Fig. B-3 Thermocouple calibrations

List of Symbols, Abbreviations, and Acronyms

1-D	1-dimensional
AC	alternating current
aTDC	after top dead center
SOC	start-of-combustion
TDC	top dead center

1 (PDF) DEFENSE TECHNICAL INFORMATION CTR DTIC OCA

2 (PDF) DIRECTOR US ARMY RESEARCH LAB RDRL CIO L IMAL HRA MAIL & RECORDS MGMT

1 (PDF) GOVT PRINTG OFC A MALHOTRA

6 (PDF) DIR USARL RDRL VT K MORGAN RDRL VTP L BRAVO C KWEON M SZEDLMAYER J TEMME K KIM